Analysis of piezoelectric energy harvester under modulated and filtered white Gaussian noise

Energy harvesting from earthquake for experimental seismic assessment of structures

31 January 2017

Abstract. The growing use of wireless sensing systems more and more often requires advanced solutions about power consumption, power management and power generation. Within this framework, recent studies have presented numerical and experimental results about self-powered wireless sensor networks for structural monitoring applications in the event of earthquake, wherein the energy is scavenged from seismic accelerations. A general computational approach for the analysis and design of energy harvesters under seismic loads, however, has not yet been presented. Therefore, this paper proposes a rational method that relies on the random vibrations theory for the electromechanical analysis of piezoelectric energy harvesters under seismic ground motion. In doing so, the ground acceleration is simulated by means of the Clough-Penzien filter. The considered piezoelectric harvester is a cantilever bimorph modeled as Euler-Bernoulli beam with concentrated mass at the free-end, and its global behavior is approximated by the dynamic response of the fundamental vibration mode only (which is tuned with the dominant frequency of the site soil). Once the Lyapunov equation of the coupled electromechanical problem has been formulated, mean and standard deviation of the generated electric energy are computed by means of an efficient semi-analytical procedure. Numerical results for piezoelectric layers made of electrospun PVDF nanofibers are discussed in order to understand issues and perspectives about the use of wireless sensor networks powered by earthquakes for the experimental seismic assessment of structures.

1. Introduction

Advances in sensing technologies and wireless transmission facilitate the installation of large sensor networks to monitor the health of civil structures and infrastructures as well as to enable their intelligent adaptation to changing conditions. On the other hand, the massive diffusion of wireless sensing systems also poses new technological challenges. Besides the search for energy-efficient solutions, the development of innovative energy harvesting solutions is expected to play a central role on the diffusion of wireless sensing systems. Amongst the emerging techniques in this field, those that aim at powering wireless sensor nodes by harvesting the energy from ambient vibrations are especially promising for civil engineering applications. In this perspective, the elaboration of effective computational strategies is as important as the experimental testing, and both are essential in order to study the feasibility of vibrations-powered sensing systems and to optimize their design.

The random vibrations theory can be a powerful methodology to analyze the electromechanical response of energy harvesters under uncertain vibrations. For instance, a single-degree-of-freedom (SDOF) electromechanical system under uncertain base motion is considered in (Adhikari et al.; 2009). Therein, the input excitation was modeled as stationary white Gaussian noise and the mean power acquired from a piezoelectric energy harvester was calculated using the theory of random vibrations. In this regards, it should be remarked that stationary random vibrations are usually relevant for civil constructions in serviceability conditions, such as for bridges under traffic load (Peigney and Siegert; 2013; Maruccio et al.; 2016). The case of non-stationary random vibrations has been addressed recently, see for instance (Yoon and Youn; 2014). Among the potential applications of energy harvesting technologies under non-stationary random vibrations, those regarding seismic events have received several attentions recently. According to (Lu et al.; 2014), the energy harvested from earthquake-induced vibrations can be used for the following important scopes:

- to power sensors designated for structural monitoring in the event of seismic loads (including the wireless transmission of recorded data to relevant agencies),
- to support active or semi-active seismic protection systems,
- to provide emergency power for the general public after an earthquake.

To date, existing literature is basically focused on the use of the energy harvested from seismic vibrations in order to supply the power required to drive a wireless network of sensors in the event of earthquake. So doing, selected devices of the sensor network harvest and accumulate the energy from earthquake-induced vibrations in their capacitors and, once sufficient energy is obtained, they will turn on their microprocessors and transceivers to perform the scheduled operations (Cheng et al.; 2013). Earthquake-powered sensing systems could be designed to operate during the strong-motion phase of the seismic event to monitor the occurrence of damages, or at its end to provide experimental data for aftershock seismic assessment of the structures. For instance, the energy generated by a piezoelectric device under seismic accelerations has been calculated in (Elvin et al.; 2006) through time-history analyses, and final results were compared with the energy obtained under traffic and wind loads. While Elvin et al. (2006) have considered an energy harvester subjected to seismic ground motion, the piezoelectric scavenger devised in (Tomicek et al.; 2013) and (Cheng et al.; 2013) gathers the energy from building motion during earthquakes. These authors have motivated such choice by observing that the frequency content of the earthquake cannot be predicted, whereas the piezoelectric energy harvesting device can be tuned at the resonant frequency of the structure on which it is mounted. This motivation, however, deserves some considerations. First, current seismological models nowadays provide a satisfactory description of the expected frequency content for most sites. On the other hand, it should be highlighted that several structures and infrastructures under intense seismic ground motion exhibit a strong nonlinear behavior which compromises the frequency tuning. If the construction is designed to behave linearly in event of

earthquake (i.e., because of proper structural details or devices for seismic protection and vibration mitigation), then the intensity of its dynamic response is typically low and the mechanical energy that can be converted into electrical energy could be insufficient to power a sensing system. In principle, harvesting the energy from earthquakes or from the seismic response of structures are, both, viable strategies, each one with its advantages and shortcomings. As a matter of fact, the selection of the final strategy to be implemented will depend on the structure to be monitored as well as on the designated scopes and features of the sensing systems. Finally, although the cited studies assume different estimates about the minimum energy required for seismic monitoring applications, all of them conclude that it is possible to power a wireless sensor node scavenging earthquake-induced vibrations. A general computational approach for the analysis and design of devices able to harvest the energy from earthquakes, however, has not yet presented.

This paper develops a general methodology based on the random vibrations theory for the analysis of piezoelectric energy harvesters under seismic accelerations. The ground motion due to the earthquake is simulated by means of the Clough-Penzien filter whereas the piezoelectric generator is a cantilever bimorph with a point mass at the free-end. It is assumed that the harvester's response is well approximated by the dynamics of the fundamental vibration mode only, which is tuned with the dominant frequency of the site soil. The non-stationary form of the Lyapunov equation is obtained by assembling the filter equations and the electromechanical equations of the piezoelectric energy harvester. Finally, mean and standard deviation of the generated electrical energy are estimated by means of an efficient semi-analytical procedure. Numerical results presented in this study are obtained for the case of piezoelectric layers made of electrospun PVDF nanofibers, and they are discussed in order to understand issues and perspectives about the use of wireless sensor networks powered by earthquakes for the experimental seismic assessment of structures.

2. Stochastic analysis of piezoelectric energy harvester under seismic ground acceleration

2.1. Stochastic model of the seismic base motion

In the context of random vibration theory, earthquake excitation is often modeled by filtering a white Gaussian noise. The most commonly adopted filtering techniques are based on the Kanai-Tajimi filter and the Clough-Penzien filter. Some applications in earthquake engineering of the filtering technique can be found, for instance, in (Marano, Trentadue and Greco; 2007; Marano, Greco, Trentadue and Chiaia; 2007; Marano, Morrone and Quaranta; 2009; Marano, Quaranta and Greco; 2009). The Kanai-Tajimi model employs a single linear filter and well approximates the high frequencies of real earthquakes, but it is less accurate for low frequencies. The latter problem has been mitigated in the Clough-Penzien filter, which takes the Kanai-Tajimi response as the

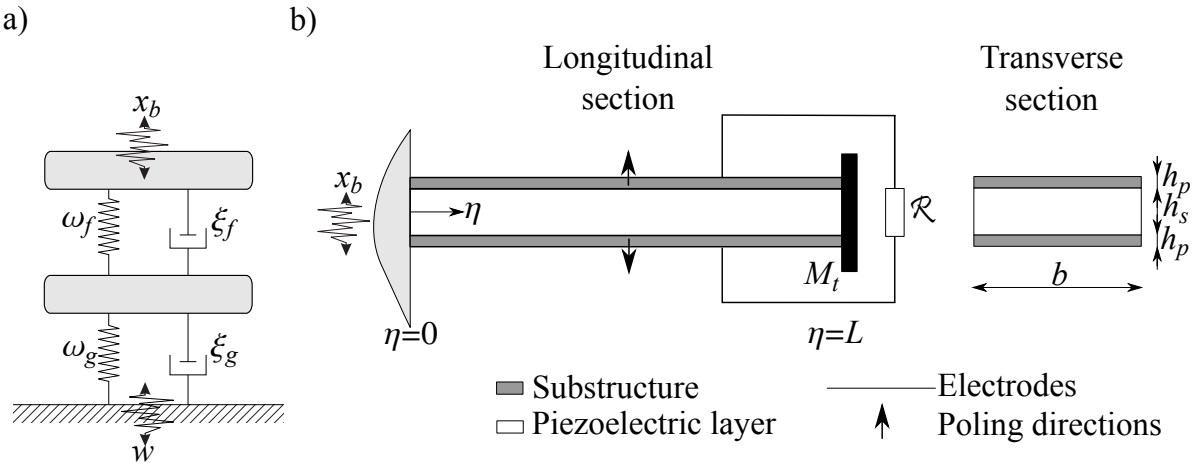

Figure 1. Considered models of a) seismic loading and b) bimorph cantilever with series connection of piezoelectric layers.

input of another linear (high-pass) filter. Specifically, in the Clough-Penzien model (Figure 1a), the base motion $\ddot{x}_b$ is given as (Neckel and Rupp; 2013):

$$\ddot{x}_b = \ddot{x}_f = -2\xi_f\omega_f\dot{x}_f - \omega_f^2 x_f - 2\xi_g\omega_g\dot{x}_g - \omega_g^2 x_g, \tag{1}$$

where x_g and x_f are the solutions of the following coupled stochastic oscillators:

$$\begin{cases} \ddot{x}_g + 2\xi_g\omega_g\dot{x}_g + \omega_g^2 x_g = -\varphi w \\ \ddot{x}_f + 2\xi_f\omega_f\dot{x}_f + \omega_f^2 x_f = -2\xi_g\omega_g\dot{x}_g - \omega_g^2 x_g \end{cases} \tag{2}$$

under zero initial conditions. Here, ω_g, ω_f, ξ_g and ξ_f are the filter parameters (ω_g and ω_f are the filters' natural frequencies whereas ξ_g and ξ_f are the filters' damping ratios). Specifically, ω_g and ξ_g are the dominant frequency and damping ratio of the site soil, respectively. On the other hand, ω_f and ξ_f denote the parameters of the filter hindering the low-frequency components of the seismic motion. In Eq. (2), φ is a time-dependent function that modulates the intensity of the zero-mean white Gaussian noise w. All filter parameters ω_g, ω_f, ξ_g and ξ_f are assumed to be time-invariant.

In real earthquakes, the dominant frequency of the site soil ω_g should be considered as time-dependent parameter (it usually decreases with the time during a seismic event). Assuming a linear time-variation, Rezaeian and Der Kiureghian (2010) estimate that its mean (negative) rate of change with the time is about 1.5% of the mean dominant frequency at the middle of the strong shaking phase. In light of this small rate of change with the time, it is believed that a constant value of ω_g is an acceptable assumption for this first study. The dominant damping ratio of the site soil ξ_g, on the contrary, is assumed as time-independent parameter in almost all studies, refer again to (Rezaeian and Der Kiureghian; 2010).

2.2. Electromechanical model of the piezoelectric energy harvester

A bimorpth energy harvester is considered with series connection of piezoelectric layers (Figure 1b). The electrode pairs on the top and on the bottom are assumed to be perfectly conductive so that a single electric potential difference can be defined across them. Their contribution to the thickness dimension is negligible. The electronic circuit consists of a resistive electrical load $\mathcal{R}$. The piezoelectric energy harvester is modeled as a continuous linear elastic Euler-Bernoulli beam following (Erturk and Inman; 2009). It is assumed that the dynamic response of the piezoelectric bimorph is dominated by its fundamental mode (which will be tuned with the dominant frequency of the site soil ω_g). The bimorph is subjected to transverse earthquake-induced accelerations $\ddot{x}_b$ at the base whereas axial motion and base rotations are not considered. Moreover, it is assumed that the tip mass M_t can be modeled as a point mass, which implies that its rotary inertia can be neglected. Under such assumptions, the equation of motion related to the considered mode is:

$$\ddot{x} + 2\xi\omega\dot{x} + \omega^2 x + \chi v = -\Lambda\ddot{x}_b. \tag{3}$$

under zero initial conditions, where x is the transverse modal mechanical response along the longitudinal axis η, v is the voltage across the resistive load $\mathcal{R}$, ξ is the modal mechanical damping ratio and ω is the undamped natural frequency of the fundamental mode in short circuit conditions (i.e., $\mathcal{R} \to 0$). Let $\phi(\eta)$ be the mass normalized eigenfunction of the fundamental vibration mode, the modal electromechanical coupling term χ in Eq. (3) reads

$$\chi = \theta \frac{\partial\phi(\eta)}{\partial\eta}\bigg|_{\eta=L}, \tag{4}$$

where θ is the piezoelectric coupling term for the series connection case. It is calculated as follows:

$$\theta = \frac{\bar{e}_{31} b}{2h_p}\left[\frac{h_s^2}{4} - \left(h_p + \frac{h_s}{2}\right)^2\right], \tag{5}$$

where $\bar{e}_{31}$ is the piezoelectric constant. Based on the plane-stress assumption, $\bar{e}_{31}$ can be given in terms of the more common piezoelectric constant d_{31} as $\bar{e}_{31} = d_{31}/s_{11}^E$ with $s_{11}^E = 1/\bar{c}_{11}^E$, where $\bar{c}_{11}^E$ is the elastic stiffness (i.e., Young's modulus) of the piezoelectric layer at constant electric field.

The term Λ in Eq. (3) is:

$$\Lambda = m\int_0^L \phi(\eta)\mathrm{d}\eta + M_t\phi(L), \tag{6}$$

where m is the mass per unit length. It is determined as follows:

$$m = b\left(\rho_s h_s + 2\rho_p h_p\right), \tag{7}$$

where ρ_s and ρ_p are the mass densities of the substructure and the piezoelectric materials, respectively. The mass normalized eigenfunction of the corresponding undamped free

vibration problem $\phi(\eta)$ is:

$$\phi(\eta) = C\left[\cos\frac{\lambda}{L}\eta - \cosh\frac{\lambda}{L}\eta + \zeta\left(\sin\frac{\lambda}{L}\eta - \sinh\frac{\lambda}{L}\eta\right)\right] \tag{8}$$

where

$$\zeta = \frac{\sin\lambda - \sinh\lambda + \lambda\dfrac{M_t}{mL}(\cos\lambda - \cosh\lambda)}{\cos\lambda + \cosh\lambda - \lambda\dfrac{M_t}{mL}(\sin\lambda - \sinh\lambda)} \tag{9}$$

and C is a modal amplitude constant which should be evaluated to fulfill the following orthogonality condition:

$$\int_0^L \phi(\eta) m \phi(\eta) \mathrm{d}\eta + \phi(L) M_t \phi(L) = 1. \tag{10}$$

The eigenvalue λ corresponding to the eigenfunction $\phi(\eta)$ in Eq. (8) is obtained by solving the characteristic equation:

$$1 + \cos\lambda\cosh\lambda + \lambda\frac{M_t}{mL}(\cos\lambda\sinh\lambda - \sin\lambda\cosh\lambda) = 0. \tag{11}$$

The natural frequency ω is:

$$\omega = \lambda^2\sqrt{\frac{EJ}{mL^4}}, \tag{12}$$

in which EJ is the bending stiffness of the bimorph

$$EJ = \frac{2b}{3}\left[E_s\frac{h_s^3}{8} + \bar{c}_{11}^E\left(\left(h_p + \frac{h_s}{2}\right)^3 - \frac{h_s^3}{8}\right)\right] \tag{13}$$

where E_s is the Young's modulus of the substructure layer.

The electric equation for the series connection of the piezoelectric layers is:

$$\dot{v} + \frac{2}{\mathcal{C}\mathcal{R}}v - \frac{2\kappa}{\mathcal{C}}\dot{x} = 0. \tag{14}$$

In Eq. (14), the capacitance $\mathcal{C}$ is determined as follows:

$$\mathcal{C} = \frac{\bar{\varepsilon}_{33}^S bL}{h_p} \tag{15}$$

where $\bar{\varepsilon}_{33}^S$ is the permittivity component at constant strain with the plane-stress assumption ($\bar{\varepsilon}_{33}^S = \varepsilon_{33}^T - d_{31}^2/s_{11}^E$, where ε_{33}^T is the permittivity component at constant stress). Finally, the modal coupling term κ in Eq. (14) is:

$$\kappa = -\frac{\bar{e}_{31}(h_p + h_s)b}{2}\left.\frac{\partial\phi(\eta)}{\partial\eta}\right|_{\eta=L}. \tag{16}$$

2.3. Response of the piezoelectric energy harvester under stochastic seismic motion

The dynamic response of the bimorph is fully described by assembling the filter's equations in Eqs. (1)–(2), the equation of motion of the bimorph in Eq. (3) and the electrical system governing equation in Eq. (14), thus obtaining:

$$\begin{cases} \ddot{x} + 2\xi\omega\dot{x} + \omega^2 x + \chi v = -\Lambda\big(- 2\xi_f\omega_f\dot{x}_f - \omega_f^2 x_f - 2\xi_g\omega_g\dot{x}_g - \omega_g^2 x_g\big) \\ \ddot{x}_g + 2\xi_g\omega_g\dot{x}_g + \omega_g^2 x_g = -\varphi w \\ \ddot{x}_f + 2\xi_f\omega_f\dot{x}_f + \omega_f^2 x_f = -2\xi_g\omega_g\dot{x}_g - \omega_g^2 x_g \\ \dot{v} + \dfrac{2}{\mathcal{RC}}v - \dfrac{2\kappa}{\mathcal{C}}\dot{x} = 0 \end{cases} . \tag{17}$$

By introducing the state-space vector:

$$\mathbf{z} = \begin{Bmatrix} x & x_g & x_f & v & \dot{x} & \dot{x}_g & \dot{x}_f \end{Bmatrix}^T , \tag{18}$$

eq. (17) reads

$$\dot{\mathbf{z}} = \mathbf{A}\mathbf{z} + \mathbf{f}, \tag{19}$$

where

$$\mathbf{A} = \begin{bmatrix} 0 & 0 & 0 & 0 & 1 & 0 & 0 \\ 0 & 0 & 0 & 0 & 0 & 1 & 0 \\ 0 & 0 & 0 & 0 & 0 & 0 & 1 \\ 0 & 0 & 0 & -\dfrac{2}{\mathcal{RC}} & \dfrac{2\kappa}{\mathcal{C}} & 0 & 0 \\ -\omega^2 & \omega_g^2\Lambda & \omega_f^2\Lambda & -\chi & -2\xi\omega & 2\xi_g\omega_g\Lambda & 2\xi_f\omega_f\Lambda \\ 0 & -\omega_g^2 & 0 & 0 & 0 & -2\xi_g\omega_g & 0 \\ 0 & -\omega_g^2 & -\omega_f^2 & 0 & 0 & -2\xi_g\omega_g & -2\xi_f\omega_f \end{bmatrix}, \tag{20a}$$

$$\mathbf{f} = \begin{Bmatrix} 0 & 0 & 0 & 0 & 0 & -\varphi w & 0 \end{Bmatrix}^T . \tag{20b}$$

3. Stochastic analysis of the output energy

3.1. Covariance analysis

The time-dependent system covariance matrix $\mathbf{R}$ of the state-space vector $\mathbf{z}$ is calculated by solving the Lyapunov equation in non-stationary condition:

$$\mathbf{A}\mathbf{R} + \mathbf{R}\mathbf{A}^T + \mathbf{B} = \dot{\mathbf{R}}, \tag{21}$$

see for instance (Trentadue and Marano; 2006). All matrices in Eq. (21) have size $n \times n$, where n is the length of the state-space vector $\mathbf{z}$ in Eq. (18) (namely, $n = 7$). The matrix $\mathbf{A}$ is given in Eq. (20a) whereas $\mathbf{B}$ has all zero elements expect $B_{6,6} = 2\pi S_0\varphi^2$. Since the filter parameters are constant data, $\mathbf{A}$ does not vary with the time whereas $\mathbf{B}$ is time-dependent because of the modulating function φ. Moreover, S_0 is the constant bilateral power density spectral function.

Although an analytical solution of Eq. (21) can be carried out using symbolic calculus, a numerical procedure is herein preferred. So doing, the time window $[0, T]$ is first divided into equal intervals by adopting a constant time step ΔT between two consecutive instants $t_{(i-1)}$ and t_i, with $i \geq 1$. Assuming a linear variation of $\dot{\mathbf{R}}$ within each time interval ΔT, ${}^{i}\mathbf{R}$ is given as:

$$ {}^{i}\mathbf{R} = {}^{(i-1)}\mathbf{R} + \frac{1}{2}\Delta T \left({}^{i}\dot{\mathbf{R}} + {}^{(i-1)}\dot{\mathbf{R}} \right), \tag{22} $$

where the suffixes $(i-1)$ and i on the left-side denote that the pertinent quantity is evaluated at the time instants $t_{(i-1)}$ and t_i, respectively. By virtue of the assumption in Eq. (22), Eq. (21) is reformulated as follows:

$$ \bar{\mathbf{A}}\,{}^{i}\mathbf{R} + {}^{i}\mathbf{R}\bar{\mathbf{A}}^{T} + \bar{\mathbf{B}} = \mathbf{0}, \tag{23} $$

where

$$ \bar{\mathbf{A}} = \frac{1}{2}\left(-\mathbf{I} + \Delta T\mathbf{A}\right), \tag{24a} $$

$$ \bar{\mathbf{B}} = \left(\mathbf{I} + \frac{1}{2}\Delta T\mathbf{A}\right) {}^{(i-1)}\mathbf{R} + \frac{1}{2}\Delta T\,{}^{(i-1)}\mathbf{R}\mathbf{A}^{T} + \frac{1}{2}\Delta T\left({}^{i}\mathbf{B} + {}^{(i-1)}\mathbf{B}\right). \tag{24b} $$

The matrices $\mathbf{0}$ and $\mathbf{I}$ in Eq. (23) and Eq. (24) are the null matrix and the identity matrix, respectively, which size is $n \times n$. Equation (23) is now the stationary form of the Lyapunov equation and it will be solved at each time instant by means of the MATLAB function "`lyap`", thus allowing the evaluation of the system covariance matrix ${}^{i}\mathbf{R}$ once ${}^{(i-1)}\mathbf{R}$ is known. In doing so, it will be assumed that ${}^{0}\mathbf{R} = \mathbf{0}$.

The output voltage v – which is required to estimate the generated electric enrgy – is a stochastic process with zero mean and time-dependent variance $\sigma_v^2 = R_{4,4}$. Besides the output voltage, the displacement response is also useful to verify the hypothesis of linear behavior and to check whether stresses and strains are compatible with mechanical strength of the materials. The displacement x is a stochastic process with zero mean and time-dependent variance $\sigma_x^2 = R_{1,1}$.

3.2. Statistical moments of the harvested energy

Following (Elvin et al.; 2006), the electrical energy is herein considered instead of the electrical power because the loading event (i.e., the seismic event) lasts a finite time length. By making explicit the time dependence through the introduction of the time variable t, the energy harvested within the time window $[0, T]$ is calculated as follows (Elvin et al.; 2006; Adhikari et al.; 2009):

$$ \mathcal{E} = \frac{1}{\mathcal{R}} \int_0^T v^2(t)\mathrm{d}t. \tag{25} $$

The first-order moment of the harvested energy is:

$$ \mathrm{E}[\mathcal{E}] = \frac{1}{\mathcal{R}} \int_0^T \mathrm{E}[v^2(t)]\mathrm{d}t = \frac{1}{\mathcal{R}} \int_0^T \sigma_v^2(t)\mathrm{d}t \tag{26} $$

where E[·] denotes the expected value operator.

The second-order statistical moment can be determined as follows:

$$\begin{aligned}\mathrm{E}\left[\mathcal{E}^2\right] =& \frac{1}{\mathcal{R}^2}\mathrm{E}\left[\left(\int_0^T v^2(t)\mathrm{d}t\right)^2\right]\\ =& \frac{1}{\mathcal{R}^2}\mathrm{E}\left[\int_0^T\int_0^T v^2(t')v^2(t'')\mathrm{d}t'\mathrm{d}t''\right]\\ =& \frac{1}{\mathcal{R}^2}\int_0^T\int_0^T \mathrm{E}\left[v^2(t')v^2(t'')\right]\mathrm{d}t'\mathrm{d}t''.\end{aligned} \tag{27}$$

Since $v(t')$ and $v(t'')$ are Gaussian variables, the integrand in Eq. (27) is:

$$\begin{aligned}\mathrm{E}[v^2(t')v^2(t'')] =& \int_{-\infty}^{\infty}\int_{-\infty}^{\infty} v^2(t')v^2(t'')\psi\left(v(t'),v(t'')\right)\mathrm{d}v(t')\mathrm{d}v(t'')\\ =& \sigma_v^2(t')\sigma_v^2(t'') + 2\mathrm{E}\left[v(t')v(t'')\right]^2\\ =& \sigma_v^2(t')\sigma_v^2(t'') + 2\Sigma_v^2(t',t''),\end{aligned} \tag{28}$$

where $\psi\left(v(t'),v(t'')\right)$ is the joint probability density function of $v(t')$ and $v(t'')$ whereas $\Sigma_v(t',t'') = \mathrm{E}\left[v(t')\,v(t'')\right]$ is the autocorrelation function, which must be calculated to evaluate the second-order statistical moment of the harvested energy. To this end, let t and $t+\tau$ be two time instants (with $\tau > 0$), the state-space formulation of the motion equation in Eq. (19) at the time instant $t+\tau$ is:

$$\frac{\partial}{\partial\tau}\mathbf{z}(t+\tau) = \mathbf{A}\mathbf{z}(t+\tau) + \mathbf{f}(t+\tau), \tag{29}$$

from which

$$\left(\frac{\partial}{\partial\tau}\mathbf{z}(t+\tau)\right)\mathbf{z}^T(t) = \mathbf{A}\mathbf{z}(t+\tau)\mathbf{z}^T(t) + \mathbf{f}(t+\tau)\mathbf{z}^T(t). \tag{30}$$

By applying the expected value operator to both sides of Eq. (30), it is found:

$$\frac{\partial}{\partial\tau}\mathrm{E}\left[\mathbf{z}(t+\tau)\mathbf{z}^T(t)\right] = \mathbf{A}\mathrm{E}\left[\mathbf{z}(t+\tau)\mathbf{z}^T(t)\right] + \mathrm{E}\left[\mathbf{f}(t+\tau)\mathbf{z}^T(t)\right]. \tag{31}$$

Since $\tau > 0$ and w is a white Gaussian noise:

$$\begin{aligned}\mathrm{E}\left[\mathbf{f}(t+\tau)\mathbf{z}^T(t)\right] =& \mathrm{E}\left[\mathbf{f}(t+\tau)\int_0^t\left(e^{\mathbf{A}(t-\vartheta)}\mathbf{f}(\vartheta)\right)^T\mathrm{d}\vartheta\right]\\ =& \int_0^t \mathrm{E}\left[\mathbf{f}(t+\tau)\mathbf{f}^T(\vartheta)\right]\left(e^{\mathbf{A}(t-\vartheta)}\right)^T\mathrm{d}\vartheta = 0.\end{aligned} \tag{32}$$

Therefore, Eq. (31) reduces to:

$$\frac{\partial}{\partial\tau}\mathbf{\Sigma}_{\mathbf{z}}(t+\tau,t) = \mathbf{A}\mathbf{\Sigma}_{\mathbf{z}}(t+\tau,t), \tag{33}$$

where $\mathbf{\Sigma}_{\mathbf{z}}(t+\tau,t) = \mathrm{E}\left[\mathbf{z}(t+\tau)\mathbf{z}^T(t)\right]$. It is highlighted that Eq. (33) is the differential equation governing the evolution of the unknown $\mathbf{\Sigma}_{\mathbf{z}}$ depending on the variable τ while

t is a given parameter. For each given value of t, therefore, Eq. (33) must be solved by assuming the following initial condition at $\tau = 0$:

$$\mathbf{\Sigma}_{\mathbf{z}}(t,t) = \mathbf{R}(t). \tag{34}$$

Once Eq. (33) is solved, the autocorrelation function $\Sigma_v(t',t'') = \mathrm{E}\left[v(t')v(t'')\right]$ in Eq. (28) can be determined. Specifically, $\Sigma_v(t',t'') = \left[\mathbf{\Sigma}_{\mathbf{z}}(t',t'')\right]_{4,4}$. It should be observed that the numerical evaluation of $\mathrm{E}\left[\mathcal{E}^2\right]$ through Eq. (27) and Eq. (28) requires the solution of Eq. (33) for a large number of time instants t. Hence, an alternative strategy is proposed to alleviate the overall computational effort. The autocorrelation function is first determined as follows:

$$\mathbf{\Sigma}_{\mathbf{z}}(t+\tau,t) = \sum_{\alpha=1}^{n=7}\sum_{\beta=1}^{n=7} \mathbf{\Sigma}_{\mathbf{z}}^{(\alpha,\beta)}(\tau) R_{\alpha,\beta}(t), \tag{35}$$

where $\mathbf{\Sigma}_{\mathbf{z}}^{(\alpha,\beta)}(\tau)$ are the solutions of the linear differential equations:

$$\frac{\partial}{\partial\tau}\mathbf{\Sigma}_{\mathbf{z}}^{(\alpha,\beta)}(\tau) = \mathbf{A}\mathbf{\Sigma}_{\mathbf{z}}^{(\alpha,\beta)}(\tau), \tag{36}$$

given the initial conditions

$$\mathbf{\Sigma}_{\mathbf{z}}^{(\alpha,\beta)}(0) = \mathbf{\Gamma}^{(\alpha,\beta)} \tag{37}$$

and

$$\left[\mathbf{\Gamma}^{(\alpha,\beta)}\right]_{p,q} = \begin{cases} 1 & \text{if } (p,q) = (\alpha,\beta) \text{ or } (p,q) = (\beta,\alpha) \\ 0 & \text{otherwise} \end{cases}. \tag{38}$$

An explicit solution of Eq. (36) can be obtained. Finally, in order to evaluate numerically the integral in Eq. (27), the following sequence of time instants is considered:

$$t_i = (i-1)\frac{T}{N_t - 1}, \tag{39}$$

with $i = 1, \ldots, N_t$. So doing, the integral in Eq. (27) is approximated as follows:

$$\begin{aligned} \mathrm{E}[\mathcal{E}^2] &\approx \left(\frac{T}{\mathcal{R}(N_t-1)}\right)^2 \sum_{i=1}^{N_t}\sum_{j=1}^{N_t} \mathrm{E}\left[v^2(t_i), v^2(t_j)\right]\gamma_i\gamma_j \\ &= \left(\frac{T}{\mathcal{R}(N_t-1)}\right)^2 \sum_{i=1}^{N_t} \gamma_i \Bigg(3\sigma_v^4(t_i) \\ &+ 2\sum_{j=i+1}^{N_t} \gamma_j \left(\sigma_v^2(t_i)\sigma_v^2(t_j) + 2\Sigma_v^2(t_i,t_j)\right) \Bigg), \end{aligned} \tag{40}$$

where

$$\gamma_i = \begin{cases} \frac{1}{2} & \text{if } i = 1 \text{ or } i = N_t \\ 1 & \text{otherwise} \end{cases}. \tag{41}$$

4. Numerical analysis

4.1. Seismic data

Among the existing proposals collected in (Marano et al.; 2008) about the numerical values for the filters parameters, the ones presented in Tab. 1 are adopted.

Parameter	Value for stiff soil	Value for soft soil
Filter parameter ω_g [rad/s]	23	11.10
Filter parameter ξ_g	0.43	0.61
Filter parameter ω_f [rad/s]	2.80	2.80
Filter parameter ξ_f	0.97	0.87

Table 1. Seismic data.

Several formulations that relate the peak ground acceleration (PGA) $\ddot{x}_b^{max}$ to S_0 have been also proposed. Following (Liu et al.; 2016), the relationship used in this study is:

$$S_0 = \frac{(\ddot{x}_b^{max})^2}{\delta^2 \left[\pi\omega_g \left(2\xi_g + \frac{1}{2\xi_g}\right)\right]} \tag{42}$$

where the peak factor δ is equal to 2.8. The modulating function φ proposed by Jennings et al. (1969) is here adopted:

$$\varphi = \begin{cases} \left(\frac{t}{t_A}\right)^2 & \text{if } t < t_A \\ 1 & \text{if } t_A \leq t \leq t_B \\ e^{-\mu(t-t_B)} & \text{if } t > t_B \end{cases}, \tag{43}$$

where $[0, t_A]$ is the rise time, $[t_A, t_b]$ is the strong motion duration whereas the decay time starts at t_B. In the following, it is assumed $\ddot{x}_b^{max} =??g$, $t_A =??$, $t_B =??$ s, $\mu =??$ s^{-1} and $T =??$ s.

4.2. Electromechanical and geometrical data

Electromechanical data adopted in this numerical study are listed in Tab. 2 whereas the geometrical data are listed in Tab. 3. It is assumed that piezoelectric layers are made of electrospun PVDF nanofibers (Persano et al.; 2013). The interested reader can refer to (Persano et al.; 2014; Maruccio and De Lorenzis; 2014; Maruccio et al.; 2015) for further computational insights about piezoelectric textiles and to (Maruccio et al.; 2016) for a numerical study about their use in energy harvesting devices designated for health monitoring applications. The substructure is made of ??. The tip mass is defined in such a way that the natural frequency of the bimorph ω is equal to the dominant frequency of the site soil ω_g. So doing, $M_t =??$ g for stiff soil and $M_t =??$ g for soft soil. Moreover, it is assumed $\xi = 0.03$.

Parameter	Piezoelectric layers	Substructure
Mass density [kg/m^3]	??	??
Young's modulus [GPa]	??	??
Piezoelectric constant d_{31} [pm/V]	??	??
Permittivity $\bar{\varepsilon}_{33}^S$ [F/m]	??	??

Table 2. Electromechanical data (permittivity of the free space $\varepsilon_0 = 8.854 \times 10^{-12}$ F/m).

Parameter	Piezoelectric layers	Substructure
Length [mm]	??	??
Width [mm]	??	??
Thickness (each) [mm]	??	??

Table 3. Geometrical data.

4.3. Results

Text...

4.4. Further considerations

Text...

5. Conclusions

Text...

Acknowledgments

Text...

References

Adhikari, S., Friswell, M. I. and Inman, D. J. (2009). Piezoelectric energy harvesting from broadband random vibrations, *Smart Materials and Structures* **18**(11): 115005.

Cheng, M., Chen, Y., Wei, H. and Seah, W. (2013). Event-driven energy-harvesting wireless sensor network for structural health monitoring, *Proceedings of the 2013 IEEE 38th Conference on Local Computer Networks (LCN), Sydney (Australia).*

Elvin, N. G., Lajnef, N. and Elvin, A. A. (2006). Feasibility of structural monitoring with vibration powered sensors, *Smart Materials and Structures* **15**(4): 977 – 986.

Erturk, A. and Inman, D. (2009). An experimentally validated bimorph cantilever model for piezoelectric energy harvesting from base excitations, *Smart Materials and Structures* **18**(2): 025009.

Jennings, P., Housener, G. and Tsai, N. (1969). Simulated earthquake motions for design purpose, *Proceedings of the 4th World Conference on Earthquake Engineering* **A**(1): 145–160.

Liu, Z., Liu, W. and Peng, Y. (2016). Random function based spectral representation of stationary and non-stationary stochastic processes, *Probabilistic Engineering Mechanics* **45**: 115 – 126.

Lu, Q., Loong, C., Chang, C.-C. and Dimitrakopoulos, E. (2014). Scavenging vibration energy from seismically isolated bridges using an electromagnetic harvester, *Proceedings SPIE* **9061**: 90610I–90610I–11.

Marano, G., Greco, R., Trentadue, F. and Chiaia, B. (2007). Constrained reliability-based optimization of linear tuned mass dampers for seismic control, *International Journal of Solids and Structures* **44**(2223): 7370 – 7388.

Marano, G., Morrone, E. and Quaranta, G. (2009). Analysis of randomly vibrating structures under hybrid uncertainty, *Engineering Structures* **31**(11): 2677 – 2686.

Marano, G., Quaranta, G. and Greco, R. (2009). Multi-objective optimization by genetic algorithm of structural systems subject to random vibrations, *Structural and Multidisciplinary Optimization* **39**(4): 385–399.

Marano, G., Trentadue, F. and Greco, R. (2007). Stochastic optimum design criterion for linear damper devices for seismic protection of buildings, *Structural and Multidisciplinary Optimization* **33**(6): 441–455.

Marano, G., Trentadue, F., Morrone, E. and Amara, L. (2008). Sensitivity analysis of optimum stochastic nonstationary response spectra under uncertain soil parameters, *Soil Dynamics and Earthquake Engineering* **28**(12): 1078 – 1093.

Maruccio, C. and De Lorenzis, L. (2014). Numerical homogenization of piezoelectric textiles for energy harvesting, *Fracture and Structural Integrity* **1**(29): 49–60.

Maruccio, C., De Lorenzis, L., Persano, L. and Pisignano, D. (2015). Computational homogenization of fibrous piezoelectric materials, *Computational Mechanics* **55**(5): 983–998.

Maruccio, C., Quaranta, G., De Lorenzis, L. and Monti, G. (2016). Energy harvesting from electrospun piezoelectric nanofibers for structural health monitoring of a cable-stayed bridge, *Smart Materials and Structures* **25**(8): 085040.

Neckel, T. and Rupp, F. (2013). *Random Differential Equations in Scientific Computing*, De Gruyter Open.

Peigney, M. and Siegert, D. (2013). Piezoelectric energy harvesting from traffic-induced bridge vibrations, *Smart Materials and Structures* **22**(9): 1–11.

Persano, L., Dagdeviren, C., Maruccio, C., De Lorenzis, L. and Pisignano, D. (2014). Cooperativity in the enhanced piezoelectric response of polymer nanowires, *Advanced Materials* **26**(45): 7574–7580.

Persano, L., Dagdeviren, C., Su, Y., Zhang, Y., Girardo, S., Pisignano, D., Huang, Y. and Rogers, J. (2013). High performance piezoelectric devices based on aligned arrays of nanofibers of PVDF, *Nature Communications* **1633**: 1–4.

Rezaeian, S. and Der Kiureghian, A. (2010). Simulation of synthetic ground motions for specified earthquake and site characteristics, *Earthquake Engineering & Structural Dynamics* **39**(10): 1155–1180.

Tomicek, D., Tham, Y., Seah, W. and Rayudu, R. (2013). Vibration-powered wireless sensor for structural monitoring during earthquakes, *Proceedings of the 6th International Conference on Structural Health Monitoring of Intelligent Infrastructure (SHMII-6 2013), Hong Kong (P.R. China)*.

Trentadue, F. and Marano, G. C. (2006). Optimum reliability based design criteria for elastic structures subject to random dynamic loads, *International Journal of Structural Stability and Dynamics* **6**(4): 437–456.

Yoon, H. and Youn, B. (2014). Stochastic quantification of the electric power generated by a piezoelectric energy harvester using a timefrequency analysis under non-stationary random vibrations, *Smart Materials and Structures* **23**(4): 045035.